Battery aging-aware adaptive model predictive control based on coupled semi-empirical electro-thermal and aging models

Xabier Dorronsoro[1]*, Ricardo de Castro[2], Jorge Varela Barreras[3,4], Erik Garayalde[1] and Unai Iraola[1]

[1] Mondragon Unibertsitatea, Faculty of Engineering, Electronic and Computing Department, Loramendi 4, Mondragon 20500 Gipuzkoa, Spain
[2] University of California, Department of Mechanical Engineering, Merced, CA, USA
[3] Technical University of Catalonia, Department of Electronic Engineering, Vilanova i la Geltru, Spain
[4] Imperial College London, Department of Civil and Environmental Engineering, London, UK

ARTICLE INFO

Keywords:
Lithium-ion battery
Derating
Optimisation
Cost
Lifetime extension
Model predictive control

ABSTRACT

This paper presents an aging-rate aware adaptive weighting nonlinear model predictive control (MPC) strategy for battery energy storage systems, integrating a semi-empirical, experimentally validated electro-thermal and degradation model to account for both calendar and cycle aging factors, often neglected in conventional energy management approaches. A key contribution is the introduction of a degradation-rate based adaptive weighting method that dynamically adjusts the MPC cost function according to the battery's aging state, primarily driven by time-dependent degradation. This adaptive mechanism enables more accurate and robust control decisions across varying prediction horizons, leading to reductions in both battery degradation and total operating costs by up to 262.7% and 44.51%, respectively, compared to a standard MPC. While the adaptive approach may result in slightly higher costs when the capacity loss rate is low compared to a rule-based baseline, it consistently achieves substantial improvements in battery lifespan (up to 101.6%), supporting more sustainable and more economically efficient operation.

1. Introduction

The introduction of Sustainable Development Goals (SDG) brings about a paradigm shift in battery energy storage systems (BESS) [1]. This redefined framework gives rise to new lines of research aimed at harnessing the potential of current and future batteries.

The first of these areas of study focuses on the domain of new technologies and materials employed in battery manufacturing [2]. The objective is geared towards next generation batteries, including, the promising lithium-metal, sodium-ion and solid-state batteries [3–5]. A second line of research is targeted at exploring more precise monitoring means, with the main goal of improving battery state estimations and ensuring safety [6, 7]. In so doing, researchers seek to better observe and estimate the phenomena that occur during their operation by, for instance, developing an approach with adaptive interconnected observers for capacity estimation [8]. A third avenue of investigation, focuses on system level, with the purpose of optimizing system sizing [9]. Finally, there is a fourth path of study that delves into battery management and control systems, which is the main focus of this article. This field involves the implementation of a variety of algorithms centred on optimizing the performance and lifetime of batteries [10].

In the scope of this latest line of research, there are different management solutions that intend to extend cells' lifetime, while keeping the main measurable parameters, such as, voltage, temperature, and state of charge (SOC), within a static Safe Operating Area (SOA). Thermal management [11–13], active balancing [11, 12], reconfiguration [14–16], and hybridization [12, 17], are some of the solutions to deal with this challenge. Nevertheless, to bring about substantial lifetime and performance improvements derating strategies are also key [10].

Derating is defined as the reduction of the operating thermal and electrical stresses of components that mitigates the degradation rate and extend its expected life [18]. When it comes to batteries, new and old units can, generally, withstand different operating conditions. Therefore, as cells age, the same scenario may lead to heterogeneous aging rates and mechanisms [19]. This implies that the battery requires a dynamic SOA that may modulate the operation, according to the aging estimations and predictions at any time. In this regard, dynamic aging-aware control systems improve performance as more accurate battery models and more advanced control strategies are envisaged. That said, this system poses the challenge of increased model complexity, which adds to the computational difficulty.

*Corresponding author
E-mail adress: xdorronsoro@mondragon.edu (X. Dorronsoro[1])
ORCID(s): 0000-0002-8030-2767 (X. Dorronsoro[1])

Nomenclature

Abbreviations

BESS Battery Energy Storage System

EMS Energy Management System

MPC Model Predictive Control

P2D pseudo-two-dimensional

PV Photovoltaic

SDG Sustainable Development Goals

SOA Safety Operating Area

SOC State of Charge

SOH State of Health

Parameters & variables

$\$_{\mathrm{Bat}}$ battery cost

α aging-rate aware adaptive weighting factor

ΔQ_{Bat} cell capacity loss

ΔQ_{Cal} cell capacity loss due to calendar

ΔQ_{Cyc} cell capacity loss due to cycling

Γ_t sublinear behavior due to time

$\Gamma_{\varphi_{\mathrm{Ch}}}$ sublinear behavior due to charged capacity throughput

$\Gamma_{\varphi_{\mathrm{Tot}}}$ sublinear behavior due to overall capacity throughput

$\overline{q}$ maximum operating state of charge of the cell

$\overline{T}$ maximum operating temperature of the cell

$\overline{v_{\mathrm{c}}}$ maximum cell terminal voltage

$\$_{\mathrm{g}}$ grid energy purchase cost

N prediction horizon

Q_{BoL} cell capacity at beginning of life

Q_{EoL} cell capacity at end of life

T_{s} simulation timestep

$\underline{q}$ minimum operating state of charge of the cell

$\underline{T}$ minimum operating temperature of the cell

$\underline{v_{\mathrm{c}}}$ minimum cell terminal voltage

φ cell capacity

φ_{Ch} cell charged capacity throughput

φ_{Tot} cell overall capacity throughput

C_{th} heat capacity of the cell

h_{th} cell-ambient heat transfer coefficient

i discrete time index

J_{Bat} battery cost function

J_{g} grid energy cost function

k discrete time index

k_0 initial optimization discrete time index

k_{Cal} calendar stress factor of the cell

$k_{\mathrm{Cyc,HighT}}$ cycling stress factor of the cell at high temperatures

$k_{\mathrm{Cyc,LowT,HighSoC}}$ cycling stress factor of the cell during the charge at low temperatures and high SoC

$k_{\mathrm{Cyc,LowT}}$ cycling stress factor of the cell during the charge at low temperatures

n discrete time index

N_{p} cells is parallel

N_{s} cells is series

P_{Bat} battery power

P_{g} grid power

P_{L} household power demand

P_{PV} solar power generation

q state of charge

Q_{Bat} cell nominal capacity

R_{Bat} electrical cell resistance

t time

T_{Bat} cell operating temperature

T_{env} ambient temperature

u control variable, electrical current of the cells in this analysis

v_{c} cell terminal voltage

v_{ocv} open circuit voltage of the cell

$f_{R_{\mathrm{Ch}}}$ function for charging electrical resistance

$f_{R_{\mathrm{Dch}}}$ function for discharging electrical resistance

R_{Bat} cell electrical resistance

R_{Ch} charge electrical resistance

R_{Dch} discharge electrical resistance

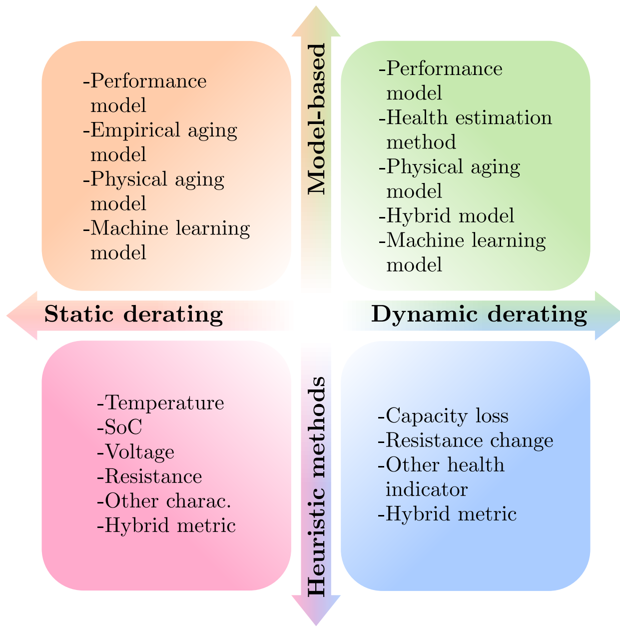

Figure 1: Battery aging-aware derating categorisation (adapted from [10]).

1.1. Literature summary

Battery derating analysis is particularly complex due to the necessity of incorporating coupled electro-thermal and aging models. The literature has attempted to address this issue through several means, being stress indicators such as temperature, SoC, voltage and electrical resistance the most standard management objectives [10]. Although these are the most commonly encountered, there is a wide variety of control alternatives calling upon a classification (such as Fig. 1) that identifies the advantages and disadvantages of each model.

On the one hand, a distinction can be drawn between static derating control strategies and dynamic derating methods. The first option involves controls that limit the operation of the battery on a steady basis, regardless of the aging process that the battery experiences. Examples include constraints of SOC [20], voltage [21] or electrical resistance [22] with constant limiting values for battery derating tasks. The latest researches introduce the use of empirical aging models to modulate the battery operation for a maximum constant aging rate value [23, 24]. The second option, classified as dynamic derating, updates the derating parameters over the life of the battery, in accordance with the estimated or predicted degradation. For instance, various researchers applied adaptive capacity loss constraints to modulate the battery operation [25, 26]. Other authors developed electrical resistance change-based [27] or physical aging model-based adaptive derating methods [28].

On the other hand, the controls can also be grouped into heuristic and model-based methods. The former concerns derating strategies that are primarily driven by a qualitative analysis of degradation and safety tests conducted in the laboratory. As evidence, a large number of studies are based on heuristics focusing on temperature [29], SOC [30], voltage[31], and electrical resistance [32]. Other authors, meanwhile, consider multiple stress factors at the same time, such as temperature and SOC in [33]. The latter relies on battery operation data to develop a model that allows estimating and/or predicting the aging and stress factors to which the battery is subjected. As an example, health estimation and prediction models are being implemented for battery control in [34]. Nonetheless, machine learning based models [35], as well as the physics based models [36] are gaining relevance for battery management according to recent publications.

Despite differences, all control models have the common goal of implementing a derating strategy aimed at extending the lifespan of the system and improving performance. In the end, better controlled battery aging rate translates into a more secure and economically competitive system [37]. As much as they strive for a common goal, they also share the shortcoming of focusing on the battery as a single unit, failing to explore the potential of the information available, not only in other agents of the system, but also in the specific application in which the battery itself has been installed. A new approach that allows dynamically contemplating the battery derating, while accounting for the rest of the system, may allow adapting the derating strategy and ensure a better impact on the performance at the system level.

A growing number of studies have attempted to formulate solutions with the aforementioned characteristics, but each approach to the problem relys on different considerations. Table 1 summarizes key examples from the literature, highlighting the characteristics of the models used, which range from electro-thermal battery models to various degradation models and control strategies characteristics. Many of these studies, such as those by Corno et al. [42] and Altaf et al. [38], focus on reducing degradation without fully integrating electro-thermal and degradation models. Schimpe et al. [23], for instance, do not consider economic impact despite including semi-empirical battery model.

More advanced solutions have recently begun utilizing MPC with the aim of taking advantage of the models information and system predictable data. However, these approaches still face various limitations. For instance, Kumar et al.'s work [48] on stochastic MPC focuses on optimizing system operation with a simplified battery model, whereas Pozzi et al. [49] use stochastic MPC for battery charging but overlook both degradation and economic costs. Li et al. [47] incorporate electro-thermal and degradation models in a nonlinear MPC but neglect battery cost, focusing only on grid cost. Similarly, Kolluri et al. [45] employ a pseudo-two-dimensional (P2D) model in nonlinear MPC to minimize battery degradation, yet without integrating economic factors from a system-wide perspective.

In summary, although numerous studies aim to advance both battery modeling and system-level optimization, the literature still presents several limitations: oversimplified battery models, weak integration between economic considerations and battery physics, and limited applicability in real-time settings. As a result, significant work remains to

Table 1
Comparative overview of proposed literature control strategies.

Author	Year	Electrical resistance	Temperature	SoC	Aging	Economic cost	Control system				Case-study
							Model-based or heuristic	Static or dynamic	Optimisation based	Prediction	
Altaf et al. [38]	2016	Yes	Yes	Yes	No	No	Model-based	Dynamic	Yes	Yes	EV
Xavier et al. [39]	2020	Yes	No	Yes	No	No	Model-based	Dynamic	Yes	Yes	EV
Keil et al. [40]	2015	No	No	No	Yes	No	Heuristic	Static	No	No	EV
Koleti et al. [41]	2019	No	No	Yes	No	No	Heuristic	Dynamic	No	No	Optimal charging
Corno et al. [42]	2020	Yes	Yes	Yes	Yes	No	Model-based	Dynamic	Yes	Yes	EV
Yin et al. [43]	2019	Yes	No	Yes	Yes	No	Model-based	Static	Yes	Yes	Fast charging
Mandli et al. [44]	2017	Yes	No	Yes	Yes	No	Model-based	Static	Yes	Yes	Fast Charging
Maheshwari et al. [37]	2020	No	No	Yes	Yes	Yes	Model-based	Dynamic	Yes	No	Grid
Sowe et al. [24]	2022	No	No	Yes	Yes	No	Model-based	Static	No	No	Grid
Kolluri et al. [45]	2020	Yes	No	Yes	Yes	No	Model-based	Dynamic	Yes	Yes	Fast charging
Tedesco et al. [46]	2022	No	No	Yes	Yes	Yes	Model-based	Dynamic	Yes	Yes	Grid
Li et al. [47]	2023	Yes	Yes	Yes	Yes	Yes	Model-based	Dynamic	Yes	Yes	Grid
Kumar et al. [48]	2019	No	No	Yes	Yes	Yes	Model-based	Dynamic	Yes	Yes	Grid
Pozzi et al. [49]	2022	Yes	Yes	Yes	No	No	Model-based	Dynamic	Yes	Yes	Fast Charging
Kumtepeli et al. [50]	2020	Yes	Yes	Yes	Yes	No	Model-based	Static	Yes	No	Grid
Schimpe et al. [23]	2021	Yes	Yes	Yes	Yes	No	Model-based	Static	No	No	Grid
This work	2024	Yes	Yes	Yes	Yes	Yes	Model-based	Dynamic	Yes	Yes	Grid

develop comprehensive solutions that accurately represent all system components without oversimplification.

1.2. Contribution of the work

Committed to overcome this obstacle, the aim of this research is to bring to the table the relevance of dynamic battery aging-aware current derating control strategies. With this goal in mind, non-linear electro-thermal and degradation models are accurately accounted for in the formulation of a novel battery energy management system (EMS). Key features such as predictability, are also taken into account. In light of the preceding, this research offers the following contributions:

- A battery aging-aware current derating strategy using an adaptive MPC framework is developed. The controller incorporates a validated semi-empirical model capturing non-linear electro-thermal dynamics and both calendar and cycle aging mechanisms, enabling enhanced battery lifespan and system performance.
- Introduces an aging-rate aware adaptive weighting mechanism that rescales the degradation cost terms in the MPC cost function at each time step. This significantly reduces the complexity of the MPC problem while preserving the accuracy required for effective long-term health optimization.
- This adaptive degradation-aware approach enables the integration of validated aging models into real-time MPC. Although demonstrated in a specific case study, the method is broadly applicable to other BESS configurations and energy management contexts.

To address the research goal, this paper is organized as follows: Section 2 introduces the models that represent the system and all the required simulation data. Section 3 presents the formulation of the baseline rule-based energy management and the predictive battery aging-aware control. Section 4 discusses the obtained results, and Section 5 outlines the main conclusions and future work.

2. System definition

Formulating and implementing a control strategy requires modeling both the system's operation and the input data related to the case-study. In this work, given that the control algorithm may take from seconds to minutes (see Section 3), the most suitable applications are those related to energy management and power balancing, where rapid response times are not critical. As illustrated in Fig. 2, the system under study is a BESS installed in a residential dwelling. Its purpose is to meet the household's energy demand with support from both the electrical grid and a photovoltaic (PV) system. Once the system model is established, the case-specific variables, along with the necessary parameters and assumptions, are defined.

2.1. System modeling

2.1.1. Power flow model

To understand the system and the basics of the control strategy, every element of the system has to be considered. The PV system supplies energy whenever generation is available, while the battery and grid collaboratively manage power flow to meet the household's energy demand. The battery operates with positive power during charging and negative during discharging, while the grid compensates for any surplus or shortfall. This relationship is governed by the power balance from Eq. 1, where P_{L} refers to the load.

$$0 = P_{\mathrm{PV}}\left[k\right] - P_{L}\left[k\right] - P_{g}\left[k\right] - P_{\mathrm{Bat}}\left[k\right] \tag{1}$$

2.1.2. Battery model

For the development of the control strategy, the cell model published by Schimpe et al. in [51, 52] is chosen. This is a physics-inspired experimentally validated semi-empirical model that captures the electrical, thermal, and degradation behavior of a commercial lithium-ion cell. For the development of the model, more than 110 cells were experimentally tested under various conditions to calibrate and validate the model, which is predictive over a wide range of SOC, temperature and current.

To scale from cell to module level, it is essential to define both the number of cell and their configuration, and

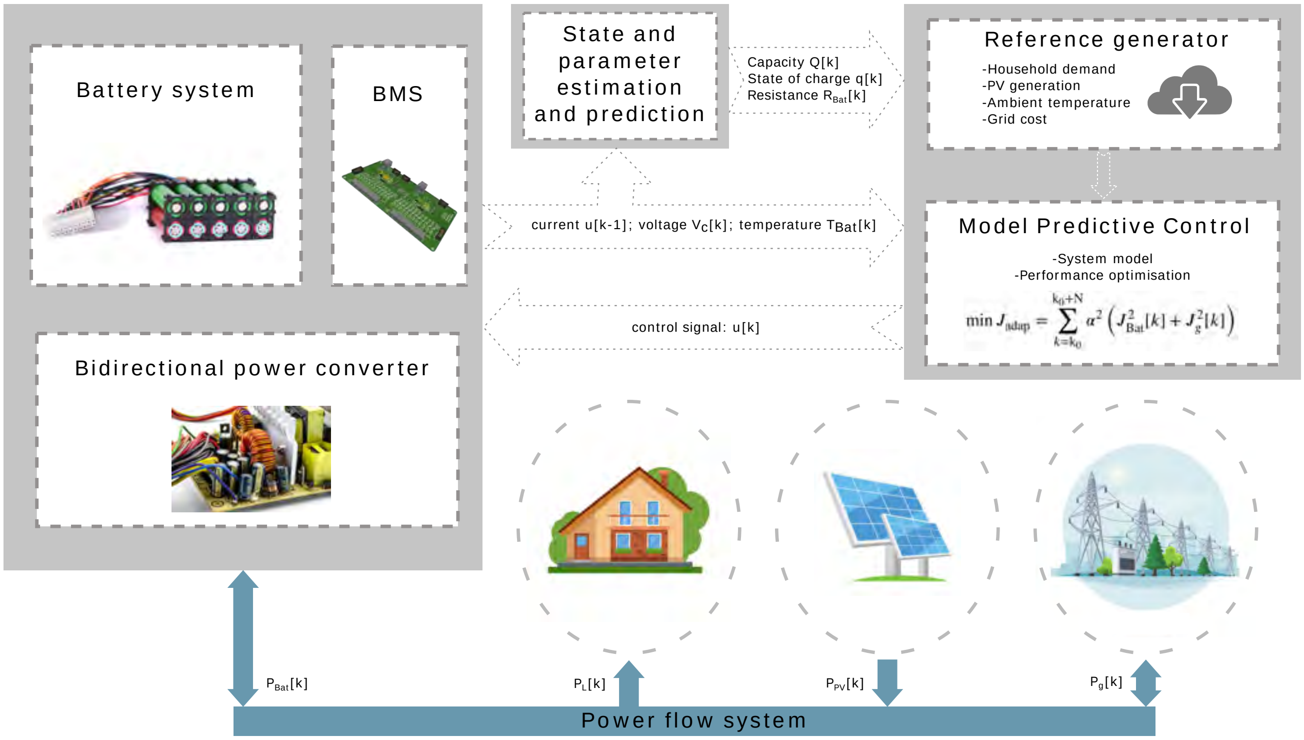

Figure 2: Overview of system configuration and the diagram of the formulated control strategy.

the individual cell model. However, two main challenges arise: modeling cell-to-cell variability and accounting for the influence of surrounding hardware (e.g., layout, balancing systems). To address these, the model assumes uniform cell behavior, supported by an active balancing system that minimizes differences between cells. Degradation effects are captured by referencing the weakest cell (defined as the one with the lowest state of health) ensuring reliable results without added computational complexity. The set of equations 2 to 9 is sourced from the work presented in [51, 52].

Regarding the electrical model, cell voltage (v_c) is based on a SOC (q) dependant open-circuit voltage source (v_{ocv}), in series with a variable voltage value that depends on a electrical current (u) and SOC and temperature dependant electrical resistor (R_{Bat}):

$$v_c[k] = v_{ocv}(q[k]) + u[k]\, R_{Bat}(T_{Bat}[k], q[k], u[k]) \quad (2)$$

To prevent severe damage, the cell's terminal voltage is kept within a safe range, between the minimum of 2.5 V ($\underline{v_c}$) and the maximum of 3.6 V ($\overline{v_c}$).

Concerning the SOC model, the control system predicts the capacity amount stored in the battery as follows,

$$q[k+1] = q[k] + \frac{\mathrm{T_s}}{Q_{Bat}}\, u[k] \quad (3)$$

where Q_{Bat} is the nominal capacity and $\mathrm{T_s}$ refers to the sample time. For safety reasons associated with overcharge and overdischarge scenarios, the operating range of q is restricted to values between $\underline{q} = 0.05$ and $\overline{q} = 0.95$.

The power delivered by the battery is calculated based on Eq. 4, scaling cell power to the size of the BESS (N_p: cells is parallel; N_s: cells in series).

$$P_{Bat}[k] = N_s\, N_p\, v_c[k]\, u[k] \quad (4)$$

For battery temperature (T_{Bat}) prediction, a simplified single cell 0D lumped thermal model is contemplated,

$$\begin{aligned} T_{Bat}[k+1] = T_{Bat}[k] + \frac{\mathrm{T_s}}{C_{th}} \Big[h_{th} \left(T_{env}[k] - T_{Bat}[k] \right) \\ + R_{Bat}(T_{Bat}[k], q[k], u[k])\, u^2[k] \Big] \end{aligned} \quad (5)$$

where T_{env} is the environmental temperature. The thermal model requires parameters such as the cell heat capacity (C_{th}), which is computed assuming the cell mass (m = 85 g) and specific heat (C_p = 838 J/kg/K). The heat transfer between the cell and the ambient is(h_{th} = 0.089 W/K) [51]. The minimum ($\underline{T_{Bat}}$) and maximum ($\overline{T_{Bat}}$) temperature constraints for the battery operation are set at -30 °C and 60 °C, respectively.

When it comes to capacity, however, as battery degradation increases, the available Ah is reduced. In order to understand how this aging evolves, Eq. 6 shows how the battery capacity loss is computed in discrete time (see Appendix A.4). Therefore, it is necessary to consider the phenomena of calendar aging and cycling aging presented in

Eq. 7, where the assessment of aging mechanisms can be conducted through superposition [52].

$$Q_{\mathrm{Bat}}[k] \approx Q_{\mathrm{Bat}}[0] - \sum_{n=1}^{k} \Delta Q_{\mathrm{Bat}}[n] \quad (6)$$

$$\Delta Q_{\mathrm{Bat}}[n] = \Delta Q_{\mathrm{Cal}}[n] + \Delta Q_{\mathrm{Cyc}}[n] \quad (7)$$

Calendar aging is estimated by summing the contributions of incremental time steps, each weighted by a temperature- and SOC-dependent degradation rate k_{Cal}, as defined in Eq. 8.

$$\Delta Q_{\mathrm{Cal}}[n] \approx \sum_{i=0}^{n} k_{\mathrm{Cal}}\big(T[i], q[i]\big)\,(\sqrt{t[i+1]} - \sqrt{t[i]}) \quad (8)$$

Cycle aging is estimated by aggregating multiple degradation mechanisms, summarized in Eq. 9, each linked to specific operating conditions: the first term captures high-temperature degradation driven by total capacity throughput (φ_{Tot}), weighted by a temperature dependent rate $k_{\mathrm{Cyc,HighT}}$; the second term accounts for degradation under low temperature conditions only during charging φ_{Ch}, and modulated by both temperature and current $k_{\mathrm{Cyc,LowT}}$; the third term addresses stress under combined low-temperature, high SOC and current conditions during the charge, weighted by $k_{\mathrm{Cyc,LowT,HighSoC}}$.

$$\begin{aligned}\Delta Q_{\mathrm{Cyc}}[n] \approx\ & \sum_{i=0}^{n} k_{\mathrm{Cyc,HighT}}\big(T_{\mathrm{Bat}}[i]\big) \\ & \cdot (\sqrt{\varphi_{\mathrm{Tot}}[i+1]} - \sqrt{\varphi_{\mathrm{Tot}}[i]}) \\ & + \sum_{i=0}^{n} k_{\mathrm{Cyc,LowT}}\big(T_{\mathrm{Bat}}[i], u[i]\big) \\ & \cdot (\sqrt{\varphi_{\mathrm{Ch}}[i+1]} - \sqrt{\varphi_{\mathrm{Ch}}[i]}) \\ & + \sum_{i=0}^{n} k_{\mathrm{Cyc,LowT,HighSoC}}\big(T_{\mathrm{Bat}}[i], q[i], u[i]\big) \\ & \cdot (\varphi_{\mathrm{Ch}}[i+1] - \varphi_{\mathrm{Ch}}[i]) \end{aligned} \quad (9)$$

2.1.3. *Economic cost model*

Having set out how the system works, it is a matter of determining the total cost. To do this, both the grid cost and the battery cost are calculated.

To predict grid cost using Eq. 10, both the grid power obtained from Eq. 1 and the grid energy purchase cost data ($\$_g$) are taken into account. In cases where energy overgeneration happens, the surplus is delivered to the grid at 0 cost (represented by the operator $\mathbf{1}_{\{P_g[k]>0\}}$).

$$J_g[k] = \$_g[k]\, T_s\, P_g[k]\, \mathbf{1}_{\{P_g[k]>0\}} \quad (10)$$

Then, it is necessary to predict the economic cost of the battery. To this end, based on the available capacity at beginning of life (Q_{BoL}) and end of life (Q_{EoL}), and the initial economic investment of the battery ($\$_{\mathrm{Bat}}$; 2.8 \$/Ah), the cost per Ah lost is established [53]. As a result, in applying Eq. 11 the corresponding battery cost is predicted.

$$J_{\mathrm{Bat}}[k] = \Delta Q_{\mathrm{Bat}}[k] \left(\frac{\$_{\mathrm{Bat}}}{Q_{\mathrm{BoL}} - Q_{\mathrm{EoL}}} \right) \quad (11)$$

2.2. System data

To analyze the performance of a control system, it is first necessary to identify the key variables that characterize the scenario, and then to define the profiles that describe their evolution over time. There are four predictable variables in this scenario and the profiles used for each one of them are shown in Fig. 3:

- Household power (P_L): a daily profile representing the monthly average (month: October) is calculated on the basis of [54]. An annual energy demand of 5000 kWh [55] is, likewise, defined.
- Solar power (P_{PV}): data on radiation is extracted from [56], in order to generate a daily profile representing the monthly average (location: Sacramento, CA, USA). The power peak of the installation is 10 kW [23].
- Ambient temperature (T_{env}): a daily profile representing the average for the month is generated based on the data from [56].
- Grid cost ($\$_g$): Based on the monthly average, a daily profile is created, taking as a reference data obtained from [57].

Additionally to these four variables, a series of parameters related to the battery are required. In this case, following the example in [23], it is a 2.5 kWh battery (with a 16P16S cell configuration). The rest of the electro-thermal and aging parameters are available in [51, 52]. On top of these data, four assumptions have been made for the initialization of the battery in each simulation:

- Assumption 1: In modeling the battery, it is undertaken that all cells operate in the same way, without heterogeneity. This assumption is supported by the presence of an balancing system, which minimizes differences in state of charge and temperature across cells. Additionally, by referencing the weakest cell (the one with the lowest state of health) throughout the analysis, the model accounts for the battery pack life limiting unit, without introducing additional computational burden.
- Assumption 2: Since all the battery's prior aging history is unknown, it is only possible to define time and capacity throughput, but not degradation-related capacity loss. Therefore, an initial state of health (SOH) of 1 is assumed for the start of all simulations.

Table 2
Cell parameters initialisation at different aging stages.

Parameters	Day 1	Week 1	Month 1	Month 6	Year 1	Year 2
φ_{Ah} [Ah]	3	21	90	480	1080	2160
φ_{Tot} [Ah]	6	42	180	960	2160	4320
t [h]	24	168	720	4320	8640	17280
SOC [%]	0.5	0.5	0.5	0.5	0.5	0.5
SOH [%]	1	1	1	1	1	1

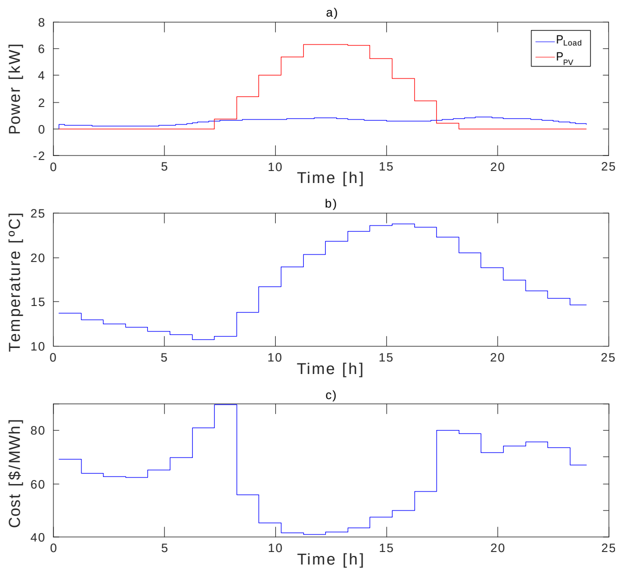

Figure 3: Predictable data for the MPC; a) Power profiles, b) Ambient temperature, c) Grid cost.

- Assumption 3: To simulate different stages in the battery's life, it is assumed that the system undergoes one full charge-discharge cycle per day with 100% efficiency. Based on this assumption, the initialization data for each simulation scenario are provided in Table 2.
- Assumption 4: Each optimization process is initialized with a current guess derived from the solution of the previous time step, serving as a warm-start to improve computational efficiency.

Finally, the main data related to the optimisation tool is required. This is specified in Table 3 (see also adaptations in Appendix A). Note also, that simulation tools are Matlab and Yalmip [58].

3. Control formulation

The literature review in Section 1.1 highlights a significant gap in existing BESS derating strategies. To address this, the present work proposes a model-based dynamic derating control approach that considers not only the battery model but the overall system behavior. This is implemented through a battery aging-aware energy management strategy using a MPC algorithm, designed to minimize the total economic cost of system operation. Given the numerical challenges that can arise when incorporating battery capacity degradation into the MPC formulation (due to the complexity of the aging model) two alternative control formulations are analyzed, named static MPC and adaptive MPC. To benchmark their performance, a rule-based energy management strategy is also considered. This comparative analysis provides insight into the control dynamics and enables a quantitative evaluation of the proposed approaches against a baseline.

Table 3
Optimisation problem parameters.

Parameters	Value
Optimisation solver	IPOPT
Prediction horizon (N)	8 and 16
Optimisation step time	15 min
Initial guess	Yes
Maximum iterations	10000
Maximum CPU time	180 s
Optimal solver tolerance	1e-12
Acceptable solver tolerance	1e-10

3.1. Battery energy management with MPC

3.1.1. Static MPC

This is a model-based dynamic derating strategy that sets the operating conditions according to the cost function defined in Eq. 12. The objective function is based on the battery cost J_{Bat} from Eq. 10 and the grid cost J_g defined in Eq. 11 along a defined prediction horizon N (where k_0 represents the initial step in the prediction window). Thus, the algorithm aims to minimize the total cost associated with the operation of the system, regulating the decision made at each time step. The quadratic cost function is chosen to enable a balanced trade-off between control effort and economic objectives, promoting stability and efficiency.

$$\min J_{\mathrm{sta}} = \sum_{k=\mathrm{k}_0}^{\mathrm{k}_0+\mathrm{N}} \left(J_{\mathrm{Bat}}^2[k] + J_g^2[k] \right) \tag{12}$$

3.1.2. Adaptive MPC

Based on the fundamentals of static MPC and considering the number of variables involved in the electro-thermal and capacity loss battery model, an increase in the complexity of formulating and solving the control problem in a stable manner can be anticipated. This hypothesis is supported by a detailed analysis of the battery's capacity loss rate dynamics. When each stress factor is examined individually, the following observations can be made:

- Stress factors: As the battery ages, the values of the aging factors, $k_{\text{Cyc,HighT}}$, $k_{\text{Cyc,LowT}}$, k_{Cal}, and $k_{\text{LowT,HighSoC}}$, remain constant and the scale does not vary over time.

- Aging dynamics: ΔQ_{Cal} and ΔQ_{Cyc} (at both high and low temperatures) exhibit a sublinear dependence on operating time, charged capacity throughput, and total capacity throughput. These sublinear terms are expressed in Eq. 13a, 13b, and 13c.

$$\Gamma_t[i] = \sqrt{t[i+1]} - \sqrt{t[i]} \tag{13a}$$

$$\Gamma_{\varphi_{\text{Tot}}}[i] = \sqrt{\varphi_{\text{Tot}}[i+1]} - \sqrt{\varphi_{\text{Tot}}[i]} \tag{13b}$$

$$\Gamma_{\varphi_{\text{Ch}}}[i] = \sqrt{\varphi_{\text{Ch}}[i+1]} - \sqrt{\varphi_{\text{Ch}}[i]} \tag{13c}$$

In view of this, to better understand the impact of the sublinear evolution of the three different aging dynamic scales on the cost function the following analyses is performed and results are shown in Fig. 4:

- The impact of time is considered in Eq. 13a by assuming a 15-minute time step over a two-year period.

- The evolution of the aging rate scale with respect to charged capacity throughput in Eq. 13b is analyzed under the assumption that one full cycle is performed each day with 100% efficiency. Based on this daily capacity initialization, the effect of different charging current rates (C/4, C/6.67 and C/20) is evaluated to observe their influence on the capacity loss scaling.

- To examine how the aging rate scaling evolves with overall capacity throughput in Eq. 13c, it is assumed that the battery completes one full charge–discharge cycle per day at 100% efficiency. Using this daily throughput reference, the influence of different current rates (C/4, C/6.67 and C/20) on capacity loss scaling is assessed.

As aging-related terms evolve over time, their contribution to the cost function may fall below the solver's tolerance, potentially hindering effective global cost optimization. In the analyzed scenario, time dependency is identified as the most limiting factor from a scaling perspective. However, identifying the system's dynamic behavior enables the introduction of an aging-rate aware adaptive weighting factor α that re-scales the problem. This scaling, defined in Eq. 14, allows the MPC to be tuned for a new battery ($\Gamma_t[1]$) such that, as aging begins ($\Gamma_t[i]$), the cost function remains properly scaled, facilitating the search for optimal operating conditions.

$$\alpha = \frac{\Gamma_t[1]}{\Gamma_t[i]} \tag{14}$$

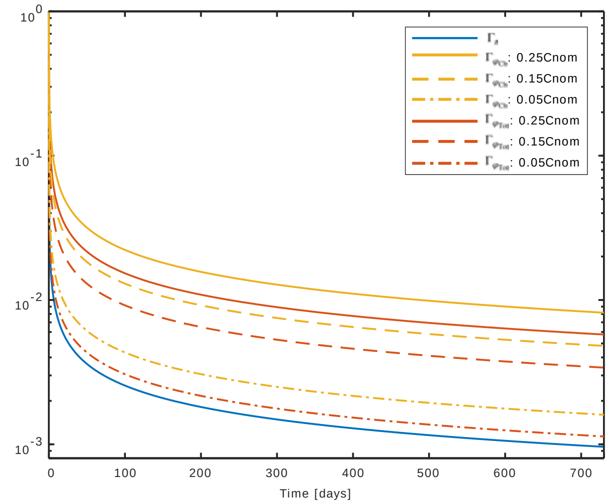

Figure 4: Capacity loss mechanism dynamics.

After identifying the potential challenge posed by the cost function defined in Eq.12, and having proposed a method to re-scale the system to avoid solver-related issues, the new cost function J_{adap} is introduced in Eq.15. In this cost function, since the dynamics related to α evolve slowly, its value is assumed to be constant in order to simplify the computational burden.

$$\min J_{\text{adap}} = \sum_{k=\text{k}_0}^{\text{k}_0+\text{N}} \alpha^2 \left(J_{\text{Bat}}^2[k] + J_g^2[k] \right) \tag{15}$$

Therefore, considering the characteristics of the power flow model, the selected battery model and the economic cost model, together with the two different MPC strategies, the problem formulation can be summarized as shown in Table 4.

3.2. Rule-based battery energy management

The rule-based battery energy management strategy is a simple and widely adopted approach in PV integrated residential energy systems, aiming to maximize self consumption of solar generation [59]. The control logic, illustrated in Fig.5, follows these principles:

- Surplus PV energy is used to charge the battery.

- Excess energy not used or stored can be exported to the grid.

- When PV generation is insufficient, the battery is discharged to meet the load.

- If both PV and battery supply are not enough, the grid provides the remaining electricity.

Table 4
Optimisation problem formulation.

Control formulation	Sub-model	Variable
Objective cost function	Static Adaptive	Eq. 12 Eq. 15
Constraints	Power v_c T_{Bat} q $\$_g$	Eq. 1 $\underline{v_c} \le v_c \le \overline{v_c}$ $\underline{T_{Bat}} \le T_{Bat} \le \overline{T_{Bat}}$ $\underline{q} \le q \le \overline{q}$ $1_{P_g[k]<0}$
State equations	v_c q P_{Bat} T_{Bat} ΔQ_{Bat} $\$$	Eq. 2 Eq. 3 Eq. 4 Eq. 5 Eq. 7 Eq. 10 and Eq. 11
Weighting factor	Static Adaptive	- Eq. 14

For a fair comparison, while maximum discharging power is based on the manufacturer limits (16.4 kW) the charging power rate is limited to 10% of its maximum charging power (245.7 W) to ensure that the battery reaches its maximum SOC by the end of the PV generation period. As seen in the results in Tab.5, this constraint enables more competitive overall performance.

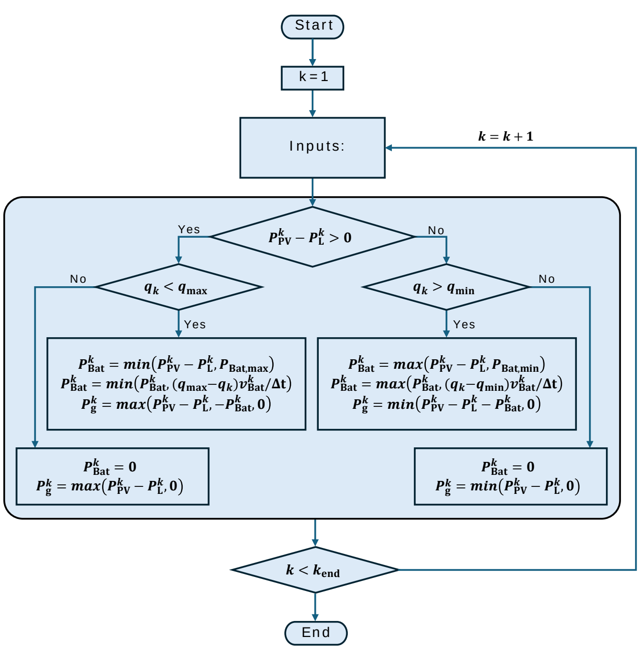

Figure 5: Rule-based energy management for the battery system (adapted from [59]).

4. Results

Building on the control strategies formulated in Section 3, the following analysis presents two main aspects. First, the dynamic behavior of the two MPC-based controllers (static vs adaptive) is compared to assess their short-term decision-making and operational performance. Then, a quantitative evaluation is carried out to compare the overall performance of all three control strategies (including the rule-based energy management) considering key metrics such as grid energy and battery cost, as well as battery degradation rate.

4.1. Comparison of MPC Control Dynamics

On the one hand, we have analysed and compared the results obtained with the static and the adaptive MPC for a single prediction horizon of N=8 steps (2 hours). In this instance, both the operating dynamics and the global results are taken into account. Additionally, different operation aging phases are factored in during the battery lifetime, as illustrated in the Tab. 2.

The Fig. 6, 7 y 8 show the operating dynamics over a 24h time period. These display how, based on the predicted power, temperature and cost profiles, both battery current and grid power are regulated in an optimal/pseudo-optimal way. From this, the following operating phases can be observed:

1. When the battery has stored energy and its use is more economical than the grid, the discharge of the BESS is prioritized. This phenomenon occurs in static and adaptive MPC.
2. If the control deems unnecessary the energy stored in the battery for the operation in the prediction horizon, it may decide to discharge it to the grid. This phenomenon occurs in the static and adaptive MPC.
3. Upon a critical increase in the cost of the grid, it is, however, observed that the system may choose to charge the battery from the grid for subsequent discharge. This phenomenon occurs in the static and adaptive MPC.
4. During periods in which the battery is discharged and is not foreseen to be needed, the most economical option is the non-use of the BESS. This is only applicable in the adaptive MPC.
5. When the system forsees a future consumption of the household and the battery is found to be a more economical option, it is opted to charge it. Always in accordance with the forecasted need of the prediction horizon. This is more accurately met in the adaptive MPC.

In this light, a system based on the adaptive MPC presents dynamics that fit more accurately the theoretical behaviour that the optimal system should display. To better understand the basics of the aging-rate aware adaptive weighting, Fig. 9 shows the impact of the adaptive factor Eq. 14 on the cost function defined in Eq.15.

That said, to determine which of the two control strategies offers better performance, it is also necessary to evaluate the results at the end of the 24 hour simulation. Fig. 10 and 11 highlight two key indicators: the capacity loss of the BESS and the total system operating cost, respectively. In all cases,

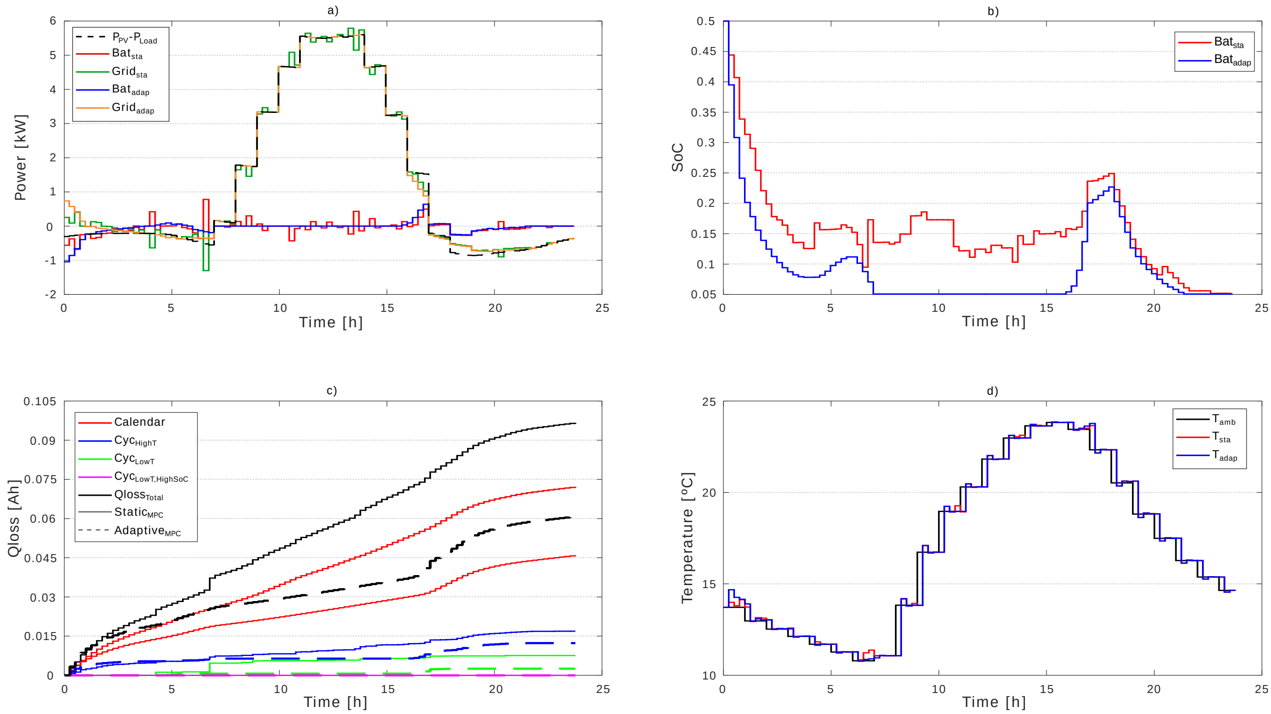

Figure 6: Static MPC vs adaptive MPC, at the first day with 2 hours of prediction horizon; a) Power profile, b) SOC, c) Capacity loss of all cells, and d) Temperature.

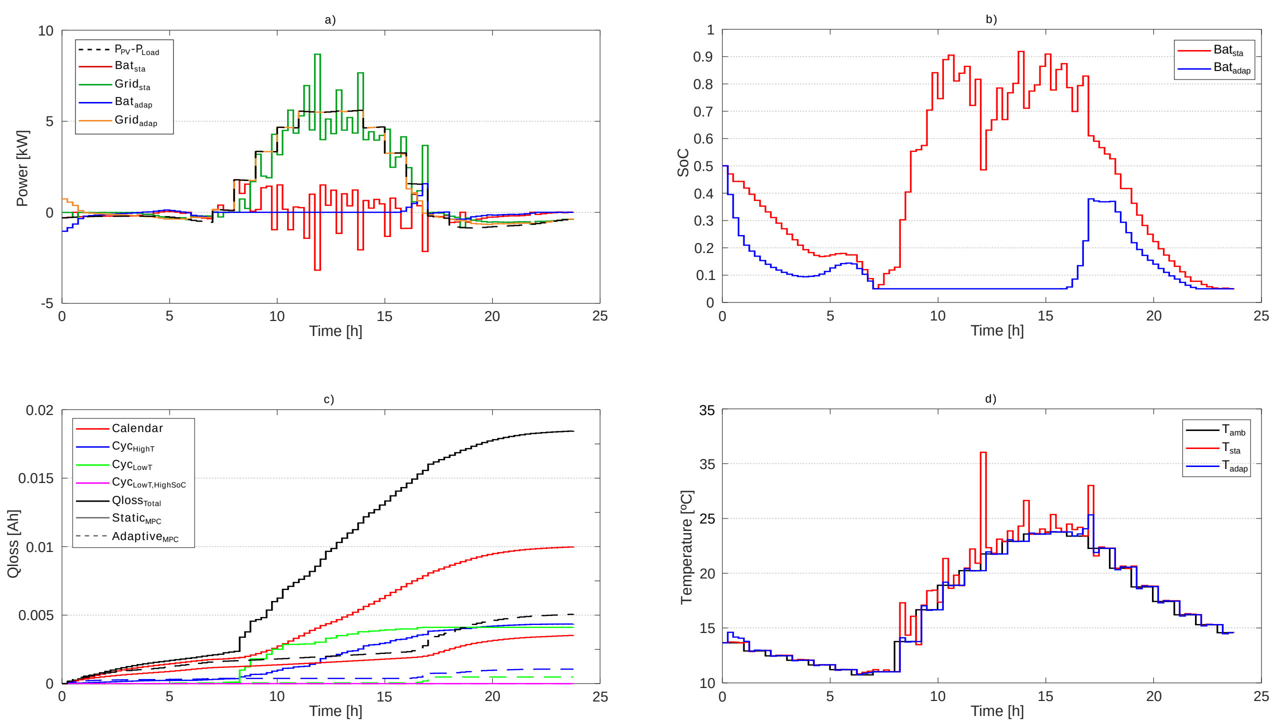

Figure 7: Static MPC vs adaptive MPC, at the first year with 2 hours of prediction horizon; a) Power profile, b) SOC, c) Capacity loss of all cells, and d) Temperature.

the adaptive control strategy reduces battery degradation (by up to 262.7%), thereby extending the battery's service life. Regarding operating costs, this reduced capacity loss results in a lower battery cost. Nevertheless, the unstable behavior of the static MPC system leads to higher SOC levels by more aggressively utilizing PV energy. As a result, once battery aging slows down, the system is able to discharge more energy, leading to lower overall costs (up to 13.7%) in certain cases. This trend is evident from the first year onward. Therefore, given that economic cost and battery degradation

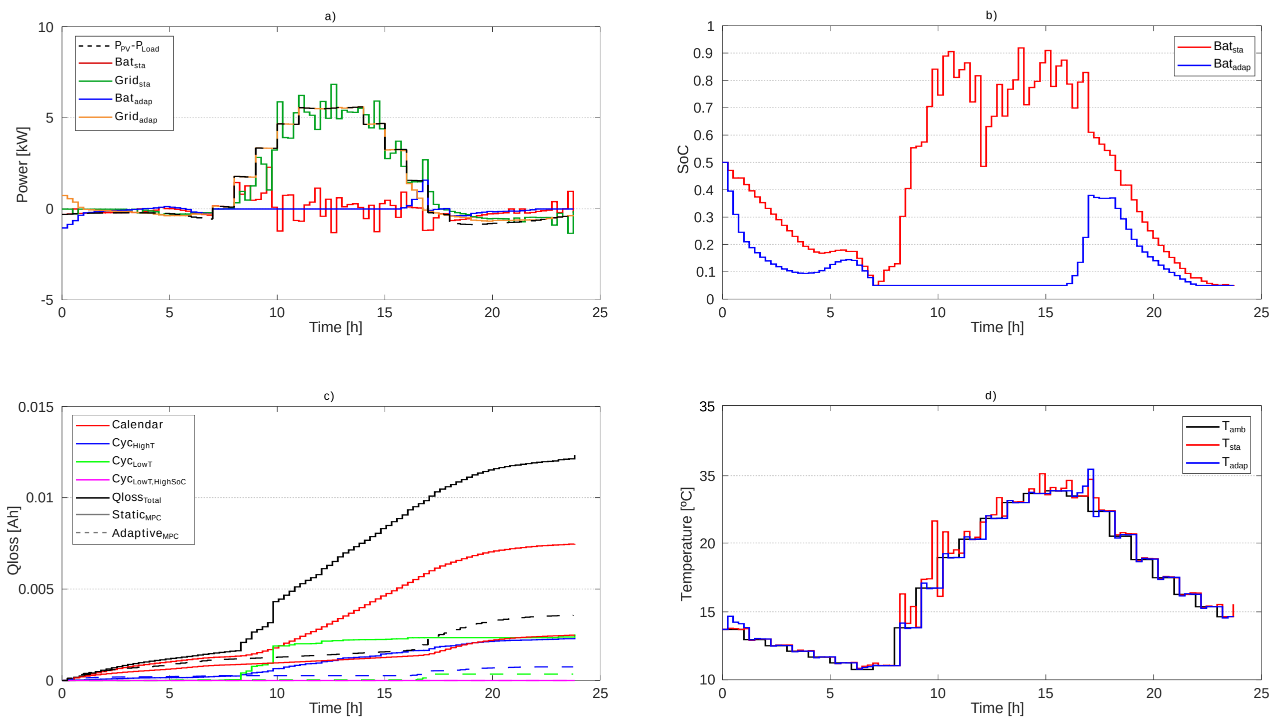

Figure 8: Static MPC vs adaptive MPC, at the second year with 2 hours of prediction horizon; a) Power profile, b) SOC, c) Capacity loss of all cells, and d) Temperature.

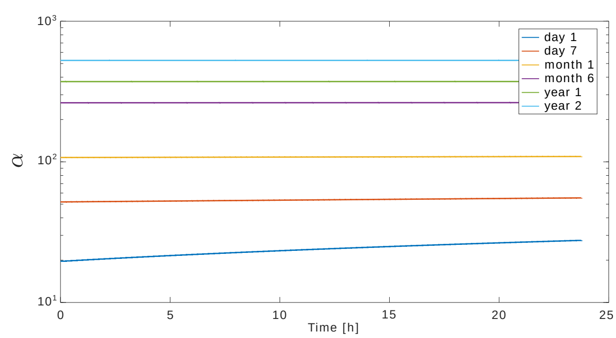

Figure 9: Adaptive weighting factor evolution over 24h simulation at different aging scenarios for N=8.

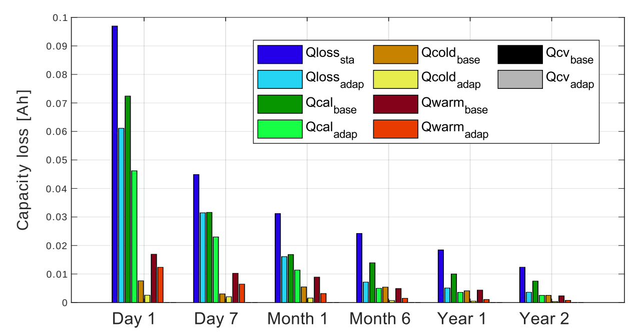

Figure 10: Static vs adaptive MPC cost comparison at different aging conditions.

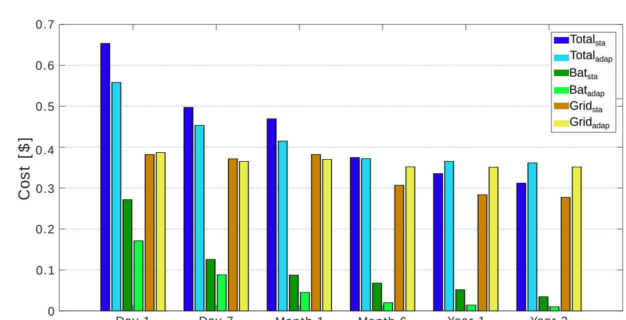

Figure 11: Static vs adaptive MPC aging comparison at different aging conditions.

are the key performance indicators, these results underscore the importance of using longer prediction horizons in adaptive control to better optimize grid usage and overall system performance.

4.2. Quantitative Evaluation of Control Strategies

Beyond the dynamic behavior of the MPC strategies, their competitiveness is evaluated by comparing performance against a rule-based control strategy (baseline), considering both economic cost and battery degradation. Additionally, the influence of the MPC prediction horizon on overall system performance indicators is analyzed. The quantitative results supporting this analysis are presented in Table 5.

When analyzing the results, battery usage is more intensive in the case of the rule-based control, due to its attempt to maximize the performance of the PV system. For the MPC alternatives, while better results are obtained with a longer prediction horizon (N=16 will be considered for comparisons), battery cycling is higher with the static MPC. These phenomena are observed across all three considered states of battery life:

- Beginning of life: Although grid cost is up to 35.8% lower with the rule-based control, the total cost is 21.7% higher compared to the adaptive MPC, which delivers the best overall performance. In the case of the static MPC, results show 4.5% lower grid cost and 13.6% higher overall cost. This is because the adaptive MPC limits battery usage to situations where it is economically beneficial compared to using grid energy, whereas the rule-based control focuses on maximizing the use of photovoltaic energy and static MPC presents unstable performance.

- After the first month: Grid costs in the static MPC and adaptive MPC cases are 51.7% and 9.8% higher, respectively, compared to the rule-based control. However, when the prediction horizon is set to N=16, battery degradation is more effectively managed. As a result, the total cost for the adaptive MPC is only 0.1% lower than that of the rule-based control, but it achieves a 20.8% reduction in battery aging, which significantly extends battery lifespan.

- After the first year: The adaptive MPC shows the worst performance in terms of grid costs 3.5% higher than the static MPC and 4.9% higher than the rule-based control. However, battery costs are lower with the adaptive MPC, being 97.9% lower compared to the static MPC and 18.9% lower than the rule-based control. Therefore, although the lowest total cost is achieved with the rule-based control by a margin of 2.5%, it comes at the expense of accelerated battery degradation.

5. Conclusions & outlook

Most existing approaches to battery management based on derating tend to overlook the complex nature of battery aging mechanisms. To address this limitation, few studies have proposed integrating degradation models and optimization strategies into aging-aware control. The novelty of this work lies in demonstrating the effectiveness of an adaptive MPC strategy that employs a aging-rate aware adaptive weighting approach for energy management in residential BESS coupled with PV generation. By dynamically scaling the control cost function according to the battery's aging state, primarily governed by time-dependent degradation, the proposed method enables more accurate and stable operation across various phases of system use. Compared to a static MPC, the adaptive approach not only extends battery lifespan but also reduces total operational costs. These improvements are further amplified when longer prediction horizons are employed.

When benchmarked against a rule-based control strategy (taken as a baseline), the adaptive MPC may result in a moderately higher total cost in the worst case (2.5%), but it achieves a substantial reduction in battery aging (18.9%). This trade-off enables more sustainable battery usage, ultimately contributing to cost-aware decision-making along the prediction horizon in pursuit of the most economically efficient scenario that extended battery lifetime.

However, it is important to recognize the limitations regarding its applicability. Due to its reliance on prediction and optimization over extended timescales, the proposed control strategy is best suited for energy management and power balancing applications that operate on a minutes-to-hours timescale. It is not appropriate for services requiring a fast response, which demand control actions within milliseconds. Additionally, since the adaptive MPC relies heavily on model accuracy for decision-making, this may present challenges in practical applications.

To further advance the analysis of the advantages and limitations of the proposed control strategy, different research directions are identified as priorities. First, it is essential to quantify the uncertainty associated with the forecasted variables and evaluate its impact on battery performance. In parallel, developing and assessing uncertainty management techniques could contribute to improving the overall economic efficiency of the system. Second, while this work considers a simplified scenario based on assumptions intended to support the interpretation of results in the context of heterogeneous battery systems, a more detailed analysis of cell-to-cell variability is necessary to understand its real influence on overall system performance (particularly under different battery configurations and balancing strategies). Finally, the integration of machine learning techniques should be explored to assess their potential in enhancing control performance and to compare them with the methods proposed in this study. This comparison may help determine whether it is more beneficial to adopt one approach over another, or even to explore the potential of a hybrid solution.

Table 5
Analysis of the different energy management systems: MPC with N=8, MPC with N=16 and rule-based control (Diff is calculated using as reference the adaptive MPC results).

		Battery at day one						
		MPC: N=8			MPC: N=16			Baseline
		Not adaptive	Adaptive	|Diff| [%]	Not adaptive	Adaptive	|Diff| [%]	Rule-based
Capacity [Ah]	Charged	304.31	161.3	88.66	435.92	271.23	60.72	691.2
	Total	953.31	668.2	42.67	1202.6	888.06	35.42	1728
Aging [Ah]	Calendar	0.0724	0.0462	56.71	0.0919	0.066	39.24	0.1346
	Cold	0.0076	0.0026	192.3	0.0068	0.0039	74.36	0.0099
	Warm	0.0169	0.0124	36.29	0.022	0.0171	28.65	0.031
	High SoC	0	0	-	0	0	-	0
	Total	0.097	0.0611	58.76	0.1207	0.087	38.74	0.1754
Cost [$]	Battery	0.2715	0.1711	58.76	0.3379	0.2435	38.74	0.4912
	Grid	0.3817	0.3867	1.3	0.3235	0.3389	4.5	0.2176
	Total	0.6532	0.5578	17.1	0.6614	0.5824	13.56	0.7088

		Battery at month one						
		MPC: N=8			MPC: N=16			Baseline
		Not adaptive	Adaptive	|Diff| [%]	Not adaptive	Adaptive	|Diff| [%]	Rule-based
Capacity [Ah]	Charged	940.01	239.47	292.5	1636.1	622.07	163	691.2
	Total	2240	824.54	171.7	3536.1	1589.7	122.4	1728
Aging [Ah]	Calendar	0.0168	0.0114	47.37	0.0251	0.0208	20.67	0.0299
	Cold	0.0055	0.0016	243.75	0.0103	0.0034	202.94	0.0021
	Warm	0.0089	0.0032	178.1	0.0146	0.0066	121.21	0.007
	High SoC	0	0	-	0	0	-	0
	Total	0.0312	0.0161	93.79	0.05	0.0309	61.81	0.039
Cost [$]	Battery	0.0874	0.0451	93.79	0.1401	0.0864	61.81	0.1092
	Grid	0.3818	0.3697	3.27	0.33	0.2389	38.13	0.2176
	Total	0.4692	0.4148	13.11	0.4701	0.3253	44.51	0.3268

		Battery at year one						
		MPC: N=8			MPC: N=16			Baseline
		Not adaptive	Adaptive	|Diff| [%]	Not adaptive	Adaptive	|Diff| [%]	Rule-based
Capacity [Ah]	Charged	1601.9	292.22	448.2	1315.3	668.59	96.73	691.2
	Total	3548.3	930.03	281.5	2973.5	1682.8	76.7	1728
Aging [Ah]	Calendar	0.01	0.0035	185.7	0.0118	0.0062	90.32	0.0087
	Cold	0.0041	0.0005	720	0.0036	0.0013	176.9	0.0006
	Warm	0.0044	0.0011	300	0.0035	0.0021	66.7	0.002
	High SoC	0	0	-	0	0	-	0
	Total	0.0185	0.0051	262.7	0.0188	0.0095	97.9	0.0113
Cost [$]	Battery	0.0517	0.0142	262.7	0.0528	0.0267	97.9	0.0318
	Grid	0.2836	0.3509	19.2	0.2208	0.2289	3.54	0.2176
	Total	0.3353	0.3651	8.16	0.2736	0.2557	7	0.2493

6. Acknowledgement

Authors would like to thank Dr Michael Schimpe from AUDI AG for sharing the battery model used in this work.

J.V.B. work is financed by the European Union - NextGenerationEU, as beneficiary of a Maria Zambrano International Talent Attraction Grant.

Appendix A Model adaptation

When developing the control algorithm, it was decided to include several adaptations to the model presented in the Section 2 in order to simplify the optimisation process while maintaining the accuracy of the results.

A.1 Power system constraints

The power flow system formulated in Eq. 1 is adapted by including the epsilon factor. This is a term that provides some flexibility to the optimisation, relaxing the calculation of the power flow with the limits set in Eq. 17.

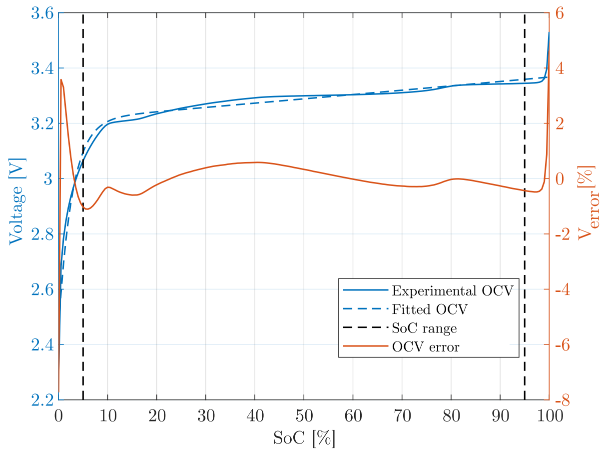

Figure 12: v_{ocv} vs SOC curve fitting.

$$\epsilon[k] = P_{\text{PV}}[k] - P_L[k] - P_g[k] - P_{\text{Bat}}[k] \tag{16}$$

$$\underline{\epsilon} \leq \epsilon[k] \leq \overline{\epsilon} \begin{cases} \overline{\epsilon} \leq 1e-3\,\text{W} \\ \underline{\epsilon} \geq -1e-3\,\text{W} \end{cases} \tag{17}$$

Limiting the operating range of the grid power based on Eq. 18 simplifies the optimisation task of the solver.

$$\underline{P_g} \leq P_g[k] \leq \overline{P_g} \begin{cases} \overline{P_g} \leq 1e4\,\text{W} \\ \underline{P_g} \geq -1e4\,\text{W} \end{cases} \tag{18}$$

A.2 Electrical resistance of the battery

The electrical resistance model (R_{Bat}), instead of operating through a switch that operates between R_{dch} and R_{ch}, is integrated using the activation function $\tanh(x)$.

$$\begin{aligned} R_{\text{Bat}}(T[k], q[k], u[k]) &= R_{\text{ch}}(T[k], q[k], u[k]) \\ &\quad + R_{\text{dch}}(T[k], q[k], u[k]) \\ R_{\text{ch}}(T[k], q[k], u[k]) &= \frac{\tanh\left(10^3 u[k]\right) + 1}{2} \\ &\quad \cdot f_{R_{\text{ch}}}\left(q[k], T[k]\right) \\ R_{\text{dch}}(T[k], q[k], u[k]) &= \frac{\tanh\left(-10^3 u[k]\right) + 1}{2} \\ &\quad \cdot f_{R_{\text{dch}}}\left(q[k], T[k]\right) \end{aligned} \tag{19}$$

A.3 Cell open circuit voltage

OCV-SOC curves were extracted via low-current step tests (C/50 at 25 °C) and fitted using a smooth polynomial (see Fig. 12), with <1.1% maximum error in the operating range.

A.4 Battery degradation model

To track degradation under real-world operation, a rate-based integral formulation is implemented, following the approach of Thomas et al. [60] and Schimpe et al. [52], enabling continuous-time aging prediction without relying on heuristic cycle counting:

$$\begin{aligned} \Delta Q_{\text{Bat}} = &\int k_{\text{Cal}}(T, q) \cdot \left(2\tau^{0.5}\right)^{-1} d\tau \\ &+ \int k_{\text{Cyc,HighT}}(T) \cdot \left(2\varphi^{0.5}\right)^{-1} d\varphi_{\text{Tot}} \\ &+ \int k_{\text{Cyc,LowT}}(T, u) \cdot \left(2\varphi^{0.5}\right)^{-1} d\varphi_{\text{Ch}} \\ &+ \int k_{\text{Cyc,LowT,High SoC}}(T, q, u)\, d\varphi_{\text{Ch}} \end{aligned} \tag{20}$$

Fig. 13 gives an overview of the stress factor correlations to cell operating conditions.

A.5 Cost model

In order to forecast the cost of the grid, it is decided to use the following equation with the aim of avoiding any *if* statement

$$J_{\text{g}} = \frac{|P_{\text{g}}[k]| - P_{\text{g}}[k]}{2} \cdot \$_{\text{g}}[k] \cdot \text{T}_{\text{s}} \tag{21}$$

References

[1] H. Kawamura, M. LaFleur, K. Iversen, H. W. J. Cheng, Frontier technology issues: Lithium-ion batteries: a pillar for a fossil fuel-free economy? (7 2021).
URL https://www.un.org/development/desa/dpad/publication/frontier-technology-issues-lithium-ion-batteries-a-pillar-for-a-fossil-fuel-fr

[2] Y. Liu, R. Zhang, J. Wang, Y. Wang, Current and future lithium-ion battery manufacturing, IScience 24 (4) (2021).

[3] B. Liu, J.-G. Zhang, W. Xu, Advancing lithium metal batteries, Joule 2 (5) (2018) 833–845.

[4] J.-Y. Hwang, S.-T. Myung, Y.-K. Sun, Sodium-ion batteries: present and future, Chem. Soc. Rev. 46 (2017) 3529–3614.

[5] J. G. Kim, B. Son, S. Mukherjee, N. Schuppert, A. Bates, O. Kwon, M. J. Choi, H. Y. Chung, S. Park, A review of lithium and non-lithium based solid state batteries, Journal of Power Sources 282 (2015) 299–322.

[6] Y. Chen, Y. Kang, Y. Zhao, L. Wang, J. Liu, Y. Li, Z. Liang, X. He, X. Li, N. Tavajohi, B. Li, A review of lithium-ion battery safety concerns: The issues, strategies, and testing standards, Journal of Energy Chemistry 59 (2021) 83–99.

[7] G. L. Plett, Battery management systems, Volume II: Equivalent-circuit methods, Artech House, 2015.

[8] A. Allam, S. Onori, Online capacity estimation for lithium-ion battery cells via an electrochemical model-based adaptive interconnected observer, IEEE Transactions on Control Systems Technology 29 (4) (2021) 1636–1651.

[9] Y. Yang, S. Bremner, C. Menictas, M. Kay, Battery energy storage system size determination in renewable energy systems: A review, Renewable and Sustainable Energy Reviews 91 (2018) 109–125.

[10] H. Ruan, J. V. Barreras, T. Engstrom, Y. Merla, R. Millar, B. Wu, Lithium-ion battery lifetime extension: A review of derating methods, Journal of Power Sources 563 (2023) 232805.

[11] J. V. Barreras, R. de Castro, Y. Wan, T. Dragicevic, A consensus algorithm for multi-objective battery balancing, Energies 14 (14) (2021).

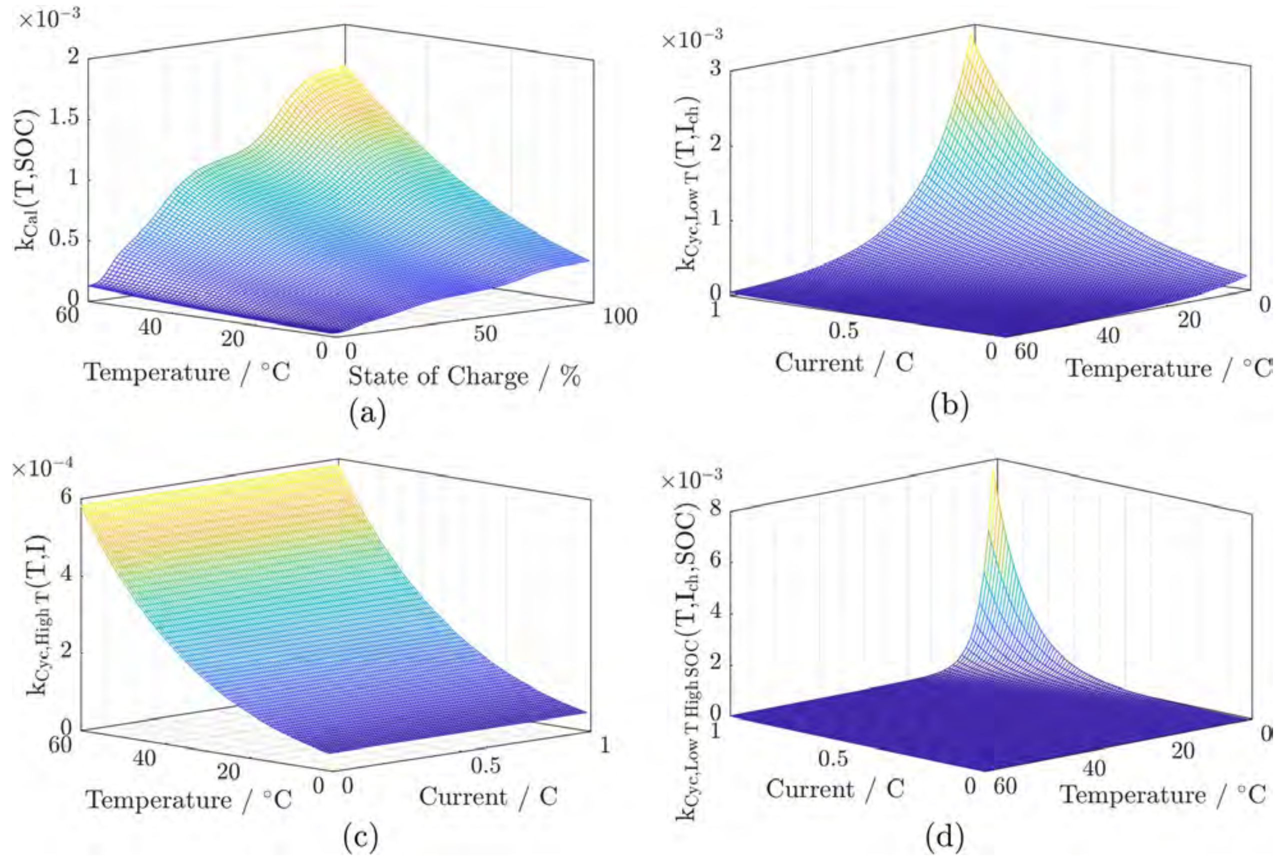

Figure 13: Evolution of the aging stress factors under different operating conditions: a) Calendar aging stress factor (Unit: $h^{-0.5}$), b) Cycling aging stess factor at different chanrging currents and temperature conditions (Unit: $Ah^{-0.5}$), c) Cycling aging stress term due to charge/discharge at different temperatures (Unit: $Ah^{-0.5}$), and d) Cycling stress factor at high SoC values when operating at different charging current and temperature conditions (Unit: Ah^{-1}) (from [52]).

[12] R. de Castro, H. Pereira, R. E. Araújo, J. V. Barreras, H. C. Pangborn, qtsl: A multilayer control framework for managing capacity, temperature, stress, and losses in hybrid balancing systems, IEEE Transactions on Control Systems Technology 30 (3) (2022) 1228–1243.

[13] D. J. Docimo, H. K. Fathy, Analysis and control of charge and temperature imbalance within a lithium-ion battery pack, IEEE Transactions on Control Systems Technology 27 (4) (2019) 1622–1635.

[14] S. Ci, N. Lin, D. Wu, Reconfigurable battery techniques and systems: A survey, IEEE Access 4 (2016) 1175–1189.

[15] S. Muhammad, M. U. Rafique, S. Li, Z. Shao, Q. Wang, X. Liu, Reconfigurable battery systems: A survey on hardware architecture and research challenges, ACM Trans. Des. Autom. Electron. Syst. 24 (2) (mar 2019).

[16] W. Han, T. Wik, A. Kersten, G. Dong, C. Zou, Next-generation battery management systems: Dynamic reconfiguration, IEEE Industrial Electronics Magazine 14 (4) (2020) 20–31.

[17] J. Cao, A. Emadi, A new battery/ultracapacitor hybrid energy storage system for electric, hybrid, and plug-in hybrid electric vehicles, IEEE Transactions on Power Electronics 27 (1) (2012) 122–132.

[18] S. (2008), Nasa/tp-2003–212242 instructions for eee parts selection,screening, qualification, and derating. URL https://nepp.nasa.gov/docuploads/FFB52B88-36AE-4378-A05B2C084B5EE2CC/EEE-INST-002_add1.pdf

[19] M. Dubarry, C. Pastor-Fernández, G. Baure, T. F. Yu, W. D. Widanage, J. Marco, Battery energy storage system modeling: Investigation of intrinsic cell-to-cell variations, Journal of Energy Storage 23 (2019) 19–28.

[20] R. Gauthier, A. Luscombe, T. Bond, M. Bauer, M. Johnson, J. Harlow, A. J. Louli, J. R. Dahn, How do depth of discharge, c-rate and calendar age affect capacity retention, impedance growth, the electrodes, and the electrolyte in li-ion cells?, Journal of The Electrochemical Society 169 (2) (2022) 020518.

[21] J. Li, J. Harlow, N. Stakheiko, N. Zhang, J. Paulsen, J. Dahn, Dependence of cell failure on cut-off voltage ranges and observation of kinetic hindrance in lini0.8co0.15al0.05o2, Journal of The Electrochemical Society 165 (11) (2018) A2682.

[22] S. S. Sebastian, B. Dong, T. Zerrin, P. A. Pena, A. S. Akhavi, Y. Li, C. S. Ozkan, M. Ozkan, Adaptive fast charging methodology for commercial li-ion batteries based on the internal resistance spectrum, Energy Storage 2 (4) (2020) e141.

[23] M. Schimpe, J. V. Barreras, B. Wu, G. J. Offer, Battery degradation-aware current derating: An effective method to prolong lifetime and ease thermal management, Journal of The Electrochemical Society 168 (6) (2021) 060506.

[24] J. Sowe, J. V. Barreras, M. Schimpe, B. Wu, C. Candelise, J. Nelson, S. Few, Model-informed battery current derating strategies: Simple methods to extend battery lifetime in islanded mini-grids, Journal of Energy Storage 51 (2022) 104524.

[25] B. Epding, B. Rumberg, M. Mense, H. Jahnke, A. Kwade, Aging-optimized fast charging of lithium ion cells based on three-electrode cell measurements, Energy Technology 8 (10) (2020) 2000457.

[26] U. R. Koleti, C. Zhang, R. Malik, T. Q. Dinh, J. Marco, The development of optimal charging strategies for lithium-ion batteries to prevent the onset of lithium plating at low ambient temperatures, Journal of Energy Storage 24 (2019) 100798.

[27] J. Sieg, J. Bandlow, T. Mitsch, D. Dragicevic, T. Materna, B. Spier, H. Witzenhausen, M. Ecker, D. U. Sauer, Fast charging of an electric vehicle lithium-ion battery at the limit of the lithium deposition process, Journal of Power Sources 427 (2019) 260–270.

[28] A. R. Mandli, S. Ramachandran, A. Khandelwal, K. Y. Kim, K. S. Hariharan, Fast computational framework for optimal life management of lithium ion batteries, International Journal of Energy Research 42 (5) (2018) 1973–1982.

[29] L. Patnaik, A. V. J. S. Praneeth, S. S. Williamson, A closed-loop constant-temperature constant-voltage charging technique to reduce charge time of lithium-ion batteries, IEEE Transactions on Industrial Electronics 66 (2) (2019) 1059–1067.

[30] J. de Hoog, J.-M. Timmermans, D. Ioan-Stroe, M. Swierczynski, J. Jaguemont, S. Goutam, N. Omar, J. Van Mierlo, P. Van Den Bossche, Combined cycling and calendar capacity fade modeling of a nickel-manganese-cobalt oxide cell with real-life profile validation, Applied Energy 200 (2017) 47–61.

[31] Y. Gao, J. Jiang, C. Zhang, W. Zhang, Z. Ma, Y. Jiang, Lithium-ion battery aging mechanisms and life model under different charging stresses, Journal of Power Sources 356 (2017) 103–114.

[32] L. Jiang, Y. Li, J. Ma, Y. Cao, C. Huang, Y. Xu, H. Chen, Y. Huang, Hybrid charging strategy with adaptive current control of lithium-ion battery for electric vehicles, Renewable Energy 160 (2020) 1385–1395.

[33] F. Altaf, B. Egardt, L. Johannesson Mårdh, Load management of modular battery using model predictive control: Thermal and state-of-charge balancing, IEEE Transactions on Control Systems Technology 25 (1) (2017) 47–62. doi:10.1109/TCST.2016.2547980.

[34] C.-H. Lee, Z.-Y. Wu, S.-H. Hsu, J.-A. Jiang, Cycle life study of li-ion batteries with an aging-level-based charging method, IEEE Transactions on Energy Conversion 35 (3) (2020) 1475–1484.

[35] T. Lombardo, M. Duquesnoy, H. El-Bouysidy, F. Årén, A. Gallo-Bueno, P. B. Jørgensen, A. Bhowmik, A. Demortière, E. Ayerbe, F. Alcaide, M. Reynaud, J. Carrasco, A. Grimaud, C. Zhang, T. Vegge, P. Johansson, A. A. Franco, Artificial intelligence applied to battery research: Hype or reality?, Chemical Reviews 122 (12) (2022) 10899–10969.

[36] A. Kawakita de Souza, W. Hileman, M. S. Trimboli, G. L. Plett, A control-oriented reduced-order model for lithium-metal batteries, IEEE Control Systems Letters 7 (2023) 1165–1170.

[37] A. Maheshwari, N. G. Paterakis, M. Santarelli, M. Gibescu, Optimizing the operation of energy storage using a non-linear lithium-ion battery degradation model, Applied Energy 261 (2020) 114360.

[38] F. Altaf, B. Egardt, L. Johannesson Mårdh, Load management of modular battery using model predictive control: Thermal and state-of-charge balancing, IEEE Transactions on Control Systems Technology 25 (1) (2017) 47–62.

[39] M. A. Xavier, A. Kawakita de Souza, G. L. Plett, M. Scott Trimboli, A low-cost mpc-based algorithm for battery power limit estimation, in: 2020 American Control Conference (ACC), 2020, pp. 1161–1166. doi:10.23919/ACC45564.2020.9147337.

[40] P. Keil, S. Schuster, C. Lüders, H. Hesse, A. Arunachala, A. Jossen, Lifetime analyses of lithium-ion ev batteries, in: 3rd Electromobility Challenging Issues conference (ECI), Singapore, 1st–4th December, 2015.

[41] U. R. Koleti, C. Zhang, R. Malik, T. Q. Dinh, J. Marco, The development of optimal charging strategies for lithium-ion batteries to prevent the onset of lithium plating at low ambient temperatures, Journal of Energy Storage 24 (2019) 100798.

[42] M. Corno, G. Pozzato, Active adaptive battery aging management for electric vehicles, IEEE Transactions on Vehicular Technology 69 (1) (2020) 258–269.

[43] Y. Yin, Y. Hu, S.-Y. Choe, H. Cho, W. T. Joe, New fast charging method of lithium-ion batteries based on a reduced order electrochemical model considering side reaction, Journal of Power Sources 423 (2019) 367–379.

[44] A. R. Mandli, S. Ramachandran, A. Khandelwal, K. Y. Kim, K. S. Hariharan, Fast computational framework for optimal life management of lithium ion batteries, International Journal of Energy Research 42 (5) (2018) 1973–1982.

[45] S. Kolluri, S. V. Aduru, M. Pathak, R. D. Braatz, V. R. Subramanian, Real-time nonlinear model predictive control (nmpc) strategies using physics-based models for advanced lithium-ion battery management system (bms), Journal of The Electrochemical Society 167 (6) (2020) 063505.

[46] F. Tedesco, L. Mariam, M. Basu, A. Casavola, M. F. Conlon, Economic model predictive control-based strategies for cost-effective supervision of community microgrids considering battery lifetime, IEEE Journal of Emerging and Selected Topics in Power Electronics 3 (4) (2015) 1067–1077.

[47] Y. Li, D. M. Vilathgamuwa, D. E. Quevedo, C. F. Lee, C. Zou, Ensemble nonlinear model predictive control for residential solar battery energy management, IEEE Transactions on Control Systems Technology 31 (5) (2023) 2188–2200.

[48] R. Kumar, J. Jalving, M. J. Wenzel, M. J. Ellis, M. N. ElBsat, K. H. Drees, V. M. Zavala, Benchmarking stochastic and deterministic mpc: A case study in stationary battery systems, AIChE Journal 65 (7) (2019) e16551.

[49] A. Pozzi, D. M. Raimondo, Stochastic model predictive control for optimal charging of electric vehicles battery packs, Journal of Energy Storage 55 (2022) 105332.

[50] V. Kumtepeli, Aging-aware battery dispatch optimization for grid applications (2020).

[51] M. Schimpe, M. Naumann, N. Truong, H. C. Hesse, S. Santhanagopalan, A. Saxon, A. Jossen, Energy efficiency evaluation of a stationary lithium-ion battery container storage system via electro-thermal modeling and detailed component analysis, Applied Energy 210 (2018) 211–229.

[52] M. Schimpe, M. E. von Kuepach, M. Naumann, H. C. Hesse, K. Smith, A. Jossen, Comprehensive modeling of temperature-dependent degradation mechanisms in lithium iron phosphate batteries, Journal of The Electrochemical Society 165 (2) (2018) A181.

[53] N. Collath, B. Tepe, S. Englberger, A. Jossen, H. Hesse, Aging aware operation of lithium-ion battery energy storage systems: A review, Journal of Energy Storage 55 (2022) 105634.

[54] M. Schlemminger, T. Ohrdes, E. Schneider, M. Knoop, Dataset on electrical single-family house and heat pump load profiles in germany, Scientific data 9 (1) (2022) 56.

[55] D. Kucevic, B. Tepe, S. Englberger, A. Parlikar, M. Mühlbauer, O. Bohlen, A. Jossen, H. Hesse, Standard battery energy storage system profiles: Analysis of various applications for stationary energy storage systems using a holistic simulation framework, Journal of Energy Storage 28 (2020) 101077.

[56] Jrc photovoltaic geographical information system (pvgis) - european commission, accessed: 08.05.2023.
URL https://re.jrc.ec.europa.eu/pvg_tools/en/

[57] Energyonline®, accessed: 08.05.2023.
URL http://www.energyonline.com/Data/GenericData.aspx?DataId=20&CAISO___Average_Price

[58] J. Löfberg, Yalmip : A toolbox for modeling and optimization in matlab, in: In Proceedings of the CACSD Conference, Taipei, Taiwan, 2004.

[59] B. Zou, J. Peng, S. Li, Y. Li, J. Yan, H. Yang, Comparative study of the dynamic programming-based and rule-based operation strategies for grid-connected pv-battery systems of office buildings, Applied Energy 305 (2022) 117875.

[60] E. Thomas, I. Bloom, J. Christophersen, V. Battaglia, Rate-based degradation modeling of lithium-ion cells, Journal of Power Sources 206 (2012) 378–382.